



# High-efficiency microstructured semiconductor neutron detectors that are arrayed, dual-integrated, and stacked

Steven L. Bellinger<sup>a,\*</sup>, Ryan G. Fronk<sup>a</sup>, Timothy J. Sobering<sup>b</sup>, Douglas S. McGregor<sup>a</sup>

<sup>a</sup> Department of Mechanical and Nuclear Engineering, Kansas State University, Manhattan, KS 66506, USA

<sup>b</sup> Electronics Design Laboratory, Kansas State University, Manhattan, KS 66506, USA

## ARTICLE INFO

Available online 25 January 2012

### Keywords:

Semiconductor neutron detectors  
Microstructured solid-state neutron detector  
He-3 replacement technology  
Microstructured diode  
Silicon wet-etching

## ABSTRACT

Silicon diodes with large aspect ratio 3D microstructures backfilled with  ${}^6\text{LiF}$  show a significant increase in neutron detection efficiency beyond that of conventional thin-film coated planar devices. Described in this work are advancements in the technology using detector stacking methods and summed-detector  $6 \times 6$ -element arraying methods to dramatically increase the sensitivity to thermal neutrons. The intrinsic detection efficiency of the  $6 \times 6$  array for normal-incident 0.0253 eV neutrons was found 6.8% compared against a calibrated  ${}^3\text{He}$  proportional counter.

© 2012 Elsevier Ltd. All rights reserved.

## 1. Introduction

Microstructured semiconductor neutron detectors (MSNDs), backfilled with neutron reactive materials, have been studied as high-efficiency thermal neutron detectors with much enthusiastic investigative work completed in the last decade (Allier, 2001; Bellinger et al., 2010a; Bellinger et al., 2010b, 2011a; Bellinger et al., 2011b; Bellinger et al., 2009a, b; Bellinger et al., 2007, 2009c; Dingley et al., 2010; Henderson et al., 2010; McGregor et al., 2007; McGregor et al., 2008; McGregor and Klann, 2003, 2007; McGregor et al., 2002; McGregor et al., 2009; McGregor and Shultis, 2011; McNeil, 2010; McNeil et al., 2006; McNeil et al., 2009a; McNeil et al., 2009b; Nikolic et al., 2010; Nikolic et al., 2007; Shultis and McGregor, 2004a; Shultis and McGregor, 2006; Shultis and McGregor, 2008, 2009; Solomon, 2007; Solomon et al., 2010; Uher et al., 2007). The basic configuration consists of a common  $pn$  junction diode, which is microstructured with an etched pattern, and then backfilled with neutron reactive materials. Such devices are compact, easily produced in mass-quantity, have low power requirements, and are far superior to common thin-film planar neutron detectors, which are restricted to low thermal neutron detection efficiencies, typically no greater than 4.5% intrinsic efficiency because of reaction production self-absorption (McGregor et al., 2003; Shultis and McGregor, 2004b). For this work, the neutron reactive material is based on the  ${}^6\text{Li}(n,t){}^4\text{He}$  reaction, such that when thermal neutrons are absorbed in  ${}^6\text{Li}$ , a 2.73 MeV triton and a 2.05 MeV helium nucleus are ejected in opposite directions (Shultis and McGregor, 2004b).

In comparison to other neutron reactive materials, the reaction products from the  ${}^6\text{Li}(n,t){}^4\text{He}$  reaction are far more energetic than those of the  ${}^{10}\text{B}(n,\alpha){}^7\text{Li}$  or  ${}^{157}\text{Gd}(n,\gamma){}^{158}\text{Gd}$  reactions, thereby improving detection and discrimination from measurable background radiation (Bellinger et al., 2010a; Shultis and McGregor, 2004b, 2009). Therefore, the following work concentrates only on devices constructed with  ${}^6\text{LiF}$  as the neutron converter material.

The present work employs the same technology, along with stacking dual-integrated  $6 \times 6$ -arrayed MSND devices to achieve unmatched solid state neutron detection sensitivity. The focus of this work involved mounting two  $6 \times 6$ -element detector chips back-to-back with counting electronics coupling them together into a single-detector modular device. For the stacked  $6 \times 6$ -arrayed MSND device, the intrinsic detection efficiency for normal incident 0.0253 eV neutrons was found by direct comparison to a calibrated  ${}^3\text{He}$  proportional counter. An important clear advantage for the 3D microstructured neutron detectors is the high efficiency achieved with a single device. Furthermore, these devices can be dual-integrated, by stacked configurations, and arrayed into a single device to dramatically increase the counting efficiency of the neutron detector.

## 2. $6 \times 6$ -Array large-area MSND design

To fabricate the dual-integrated stacked-detector for assembled large-area panel arrays, a whole  $6 \times 6$ -arrayed ( $1\text{ cm}^2$  individual elements) MSND device was manufactured on a 4-inch diameter Si wafer. Initially, an oxide is grown on a 7–14  $\text{k}\Omega\text{-cm}$   $n$ -type Si wafer in which a diffusion window is patterned. Microstructured perforations are then etched into the Si diffusion windows with a KOH wet-etch

\* Corresponding author. Tel.: +1 785 532 7087.

E-mail address: [slb3888@ksu.edu](mailto:slb3888@ksu.edu) (S.L. Bellinger).

process where the trench pattern is aligned to the  $\langle 111 \rangle$  planes in a (110) orientated Si wafer. The MSND devices reported in the present work have straight trenches etched 60  $\mu\text{m}$  deep by 25  $\mu\text{m}$  wide, where the trenches are spaced in a 50  $\mu\text{m}$  pitch, see Fig. 1. The straight trench design maintains high neutron detection efficiency while creating an opportunity to off-set stack the detector chips so as to maximize neutron absorption as reported in (Bellinger et al., 2010b). After the etch process, the wafer is chemically cleaned and  $p$ -type regions are diffused uniformly into individual device microstructures across the wafer, thereby forming conformal  $pn$  junctions within the trenches. A Ti-Al metal contact is evaporated directly on the backside of the high-resistivity wafer to make an electrical ground contact, thereby completing the diode structure and enabling depletion through the bulk of the individual devices. Finally,  $^6\text{LiF}$  powder is pushed into the microstructures by hand to function as the neutron absorbing converter material. The leakage current for an individual-element 1  $\text{cm}^2$  device was 45  $\text{nA}/\text{cm}^2$  at the reverse-bias operation voltage of 2.5 V.

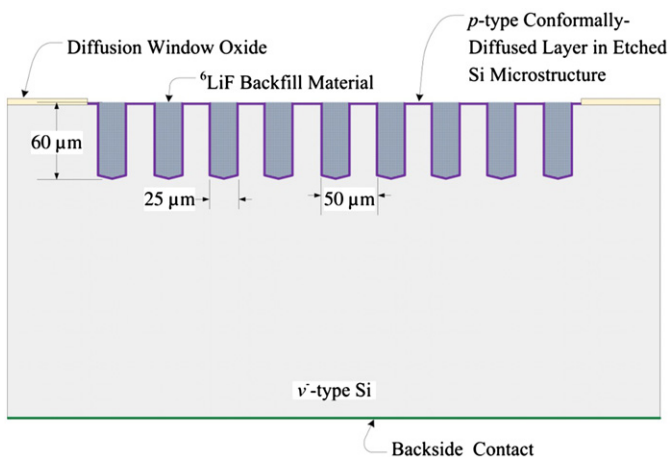


Fig. 1. Cross-section illustration of a fabricated MSND with conformally-diffused diode structure.

Two  $6 \times 6$ -arrayed MSND device chips were mounted with highly specialized dual-integrating amplifying and readout electronics, specifically designed in-house to be compact and fitted together like Legos<sup>TM</sup>, see Fig. 2. The counting electronics were designed to be packaged compactly together on 4-stacked boards (1 MSND mounting board, 2 preamplifier boards, and 1 amplifier/signal-shaping board), see Fig. 3. The motherboard and preamplification board were made from FR-4 epoxy-glass material from *Advanced Circuits* and was 762  $\mu\text{m}$  thick. The mounting board was made from FR-4 epoxy-glass material from *Advanced Circuits* and was 1,575  $\mu\text{m}$  thick. The two  $6 \times 6$ -array MSND chips were mounted back-to-back on an aluminum plated mounting board, with the preamplifier board mounted on top of each array. The mounting board provides the connection for the positive bias voltage to the common cathode on the backside of the silicon. The contact connection wires (for the 36 individual devices) are wire-bonded to the top of the MSND device chip through holes in the preamplifier board. In this configuration, the anodes of each detector are applied to the input of a charge sensitive preamp with a  $\sim 10.2 \mu\text{s}$  time constant and a nominal gain of 1.4 V/pC. A relatively short time constant is used because high counting rates are expected for some applications. The preamp board can be reconfigured such that feedback from a downstream integrator can be applied to compensate for the DC offset caused by the increased leakage currents resulting from the trenching of the detectors. Examination of the causes of higher leakage currents for the MSNDs compared to planar diode devices is studied in (Bellinger et al., 2009a). All connections to and from the preamp board are on two single-row 50-pin edge connectors. The preamplifier signals are routed to a motherboard which provides power, an adjustable +0 V to +2.5 V detector bias, pulse shaping and gain, an analog output for pulse-height analysis, and a “digital” output from a discriminator. In addition, to reduce the amount of circuitry required, four preamplifiers are connected to one shaping amplifier, see Fig. 4. The input signal is processed by a pole-zero cancellation stage with a gain of  $-56$  and time constants of 12.1  $\mu\text{s}$  (zero) and 10  $\mu\text{s}$  (pole). The discriminator output is a 3.3 V logic level that is “high” as long as the analog output is above threshold. The analog output is a semi-Gaussian pulse with a FWHM width of 18.5  $\mu\text{s}$  and a gain of  $\sim 130.2 \text{ mV}/\text{fC}$ . The input referred noise is 1.06 fC(rms). All values

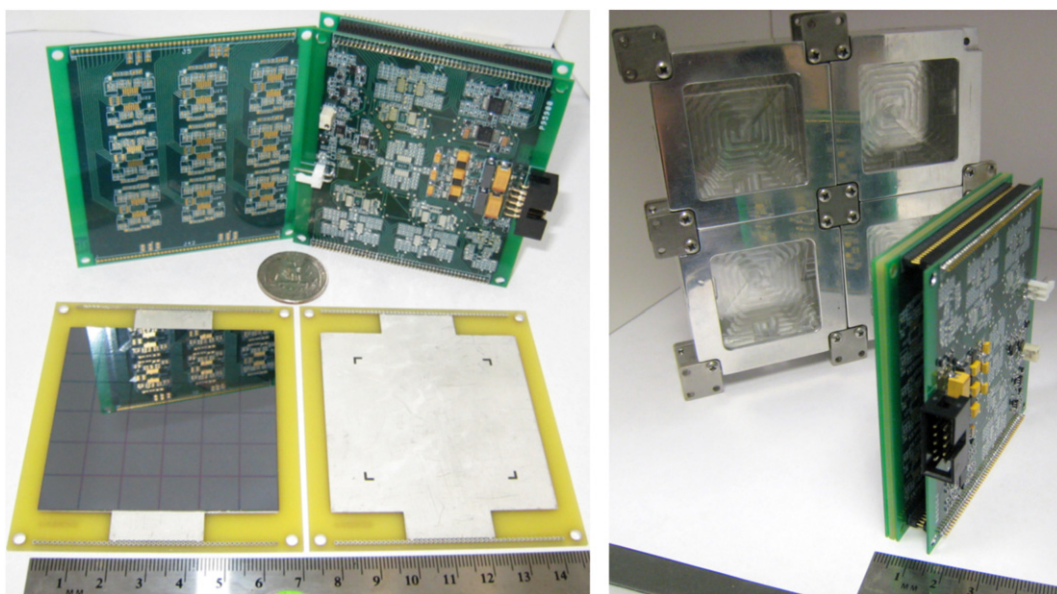
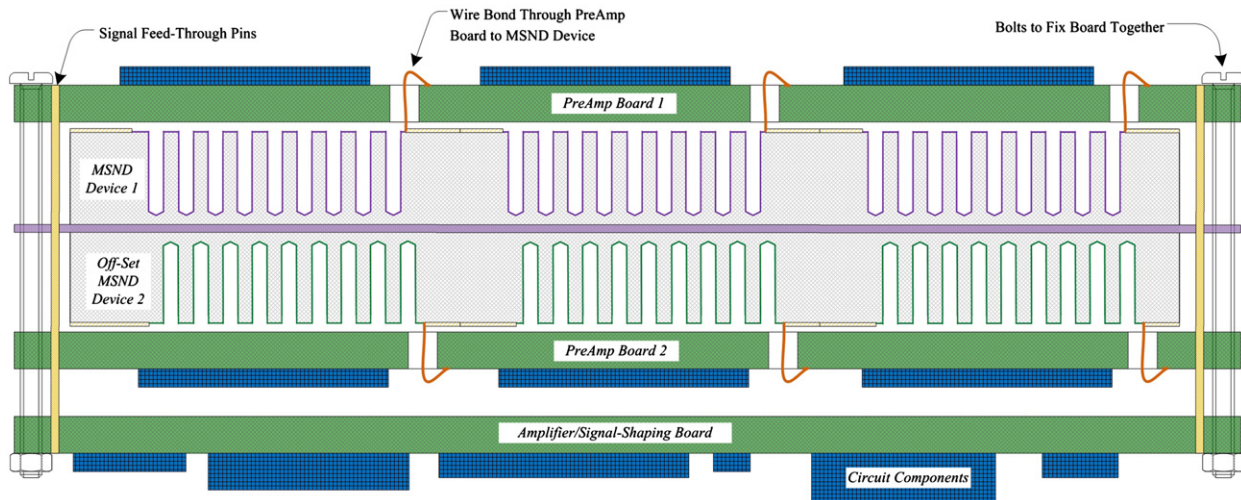
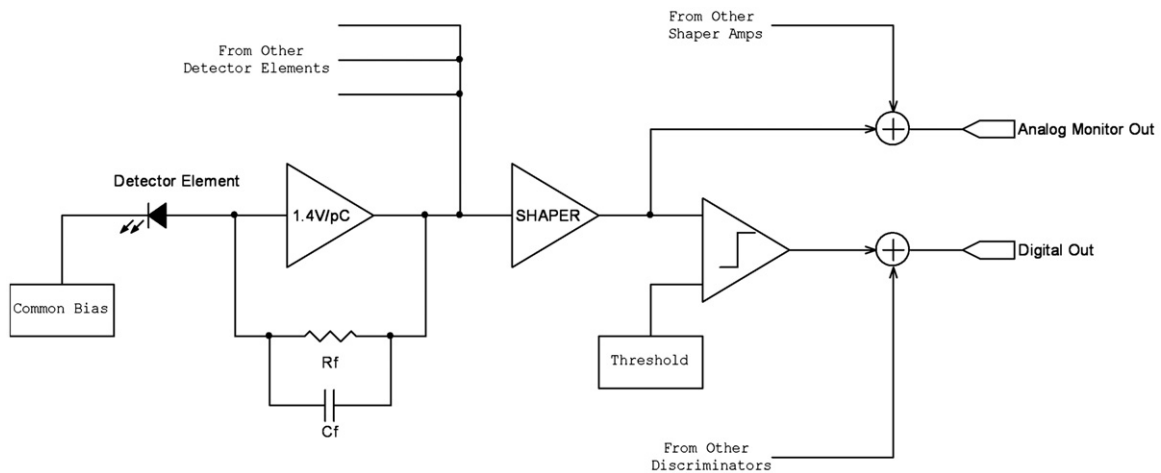


Fig. 2. (left) Shown is a disassembled dual-integrated  $6 \times 6$ -arrayed MSND device with amplifying circuitry, adjustable detector bias, bias current compensation, pulse shaping and gain, an analog output for pulse-height analysis, and a “digital” output from a discriminator. Two  $6 \times 6$  MSND arrays are mounted back-to-back, with both sides of the mounting board shown in the lower half of the picture. (right) Shown is the assembled MSND  $6 \times 6$ -array packaged device, with a characteristic aluminum housing for assembling many devices into a large detector panel array.



**Fig. 3.** Illustration of a cut-section assembly of the  $6 \times 6$ -arrayed MSND device with preamplifier board, dual-MSND array mounting board, and summed-amplifying/digitizing circuitry board. Note that for simplicity only 3 devices are shown and the MSND device scale is enlarged.



**Fig. 4.** Illustrated above is the stacked  $6 \times 6$ -element arrayed MSND device basic readout circuit schematic for pulse amplification, adjustable detector bias, pulse shaping and gain, and analog and digital output.

were measured using a 100 pF detector capacitance. The simulated detector capacitance was chosen based on measured MSND capacitance values at a detector reverse bias of 2.5 V. Overall each channel requires less than 250  $\mu$ A.

### 3. Performance of the dual-integrated large-area $6 \times 6$ -arrayed MSND

The stacked  $6 \times 6$ -element arrayed MSND device neutron-counting efficiency was measured with a 0.0253 eV diffracted neutron beam (1.25 cm diameter) from the Kansas State University TRIGA Mark II nuclear reactor (Unruh, 2009). The stacked arrayed MSND device intrinsic efficiency was measured by direct comparison to a calibrated Reuter-Stokes  $^3\text{He}$  gas-filled proportional detector, where both devices were centered in the diffracted neutron beam. Details of the  $^3\text{He}$  proportional detector calibration method can be found elsewhere (McGregor et al., 2009). Summed counts were collected from both detectors placed separately in the diffracted neutron beam. The summed count results for each device are reported in Table 1. The neutron counting efficiency was calculated by dividing the summed neutron counts, collected from the stacked  $6 \times 6$ -element arrayed MSND device with a lower level discriminator (LLD) set above the system noise, by the calibrated fluence

determined with the  $^3\text{He}$  detector. The stacked arrayed MSND device intrinsic efficiency was measured to be  $6.82 \pm 0.03\%$  as shown in Table 1. Further analog-signal output analysis from thermal- and fast-neutron detection with the  $6 \times 6$ -arrayed MSND is presented in (Bellinger et al., 2011b).

The measured thermal neutron detection intrinsic efficiency was found to be much less than the earlier calculated intrinsic efficiency found elsewhere (Shultis and McGregor, 2009). A portion of the difference may be accounted by the large neutron-streaming un-microstructured regions (0.65 mm wide) between the individual elements of the MSND array, which were not factored into the calculated intrinsic efficiency. Assuming the 1.25 cm diameter neutron-beam is centered on a single stacked-element of the array, 13.8% of the beam area does not intersect an active region of the arrayed neutron detector. In addition, thermal neutrons may be lost through absorption and scattering in the top-mounted motherboard, preamplification board, and the MSND mounting board and their respective electronic components, see Fig. 3. To verify this hypothesis, a motherboard and mounting board attenuation experiment was performed. Each board was separately placed in the diffracted thermal-neutron beam at 1 kW of power and a summed count was taken with the calibrated  $^3\text{He}$  detector with and without the board. In this way the thermal-neutron attenuation for each board was measured.

**Table 1**  
Intrinsic thermal neutron detection efficiencies for the stacked 6 × 6-element arrayed MSND device and the diffracted thermal neutron beam calibration via calibrated <sup>3</sup>He gas-tube.

Detector	Count time (s)	Summed counts	Measured intrinsic efficiency	Calculated intrinsic efficiency
Stacked 6 × 6	900	51831	6.82 ± 0.03%	18.9% (Shultis and McGregor, 2009)
<sup>3</sup> He	100	67948	80.7% (McGregor et al., 2009)	

The motherboard and preamplification board attenuated 16.8% of the beam and the mounting board attenuated 28.7% of the beam. Obviously the boards are absorbing a large number of the neutrons and should be reduced in thickness or, at least, another board type should be used that has lower neutron attenuation. Another reason for the difference between the calculated intrinsic efficiency and the measured is that the LiF powder does not pack completely solid within the microstructures. Hence, the “effective density” is less than the solid form which is what was used in the calculated predictions of the detection efficiency.

#### 4. Conclusions

A dual-integrated, stacked 6 × 6-element arrayed MSND device, backfilled with <sup>6</sup>LiF powder has been characterized for neutron sensitivity in a diffracted 0.0253 eV thermal neutron beam from a TRIGA Mark II nuclear reactor. An important clear advantage for the dual-integrated microstructured neutron detector design is the increased efficiency achieved by appropriately stacking two detector chips into a single device. These arrayed devices maybe arranged in large panel arrays for increased neutron sensitivity. Future work for these stacked arrayed-MSND devices will include reduction of the isolation barrier between devices, reduction of the motherboard and preamplification board thicknesses to reduce neutron absorption loss, and increased MSND microstructure depth to increase neutron detection efficiency per 6 × 6-element module. Additional future work will include investigation of fast neutron sensitivity in a bare <sup>252</sup>Cf neutron field at 1 m distance.

#### Acknowledgments

This work was supported in part by DTRA Contract DTRA01-02-D-0067.

#### References

Allier, C.P., 2001. Micromachined Si-well scintillator pixel detectors. DUP Science, Netherlands.

Bellinger, S.L., Fronk, R.G., McNeil, W.J., Shultis, J.K., Sobering, T.J., McGregor, D.S., 2010a. Characteristics of the Stacked Microstructured Solid-State Neutron Detector. Proc. SPIE—Int. Soc. Opt. Eng., 78016–78050.

Bellinger, S.L., Fronk, R.G., McNeil, W.J., Sobering, T.J., McGregor, D.S., 2010b. High Efficiency Dual-Integrated Stacked Microstructured Solid-State Neutron Detectors. IEEE Nucl. Sci. Sym. Conf. Rec., 2008–2012.

Bellinger, S.L., Fronk, R.G., McNeil, W.J., Sobering, T.J., McGregor, D.S., 2011a. Enhanced Variant Designs and Characteristics of the Microstructured Solid-State Neutron Detector. Nucl. Instrum. Meth. A652, 387–391.

Bellinger, S.L., Fronk, R.G., Sobering, T.J., McGregor, D.S., 2011b. Arrayed High Efficiency Dual-Integrated Microstructured Semiconductor Neutron Detectors. IEEE Nucl. Sci. Sym. Conf. Rec.

Bellinger, S.L., McNeil, W.J., McGregor, D.S., 2009a. Improved Fabrication Technique for Microstructured Solid-State Neutron Detectors, In: MRS Spring Meeting, pp. 57–65.

Bellinger, S.L., McNeil, W.J., McGregor, D.S., 2009b. Variant Designs and Characteristics of Improved Microstructured Solid-State Neutron Detectors. IEEE Nucl. Sci. Sym. Conf. Rec., 986–989.

Bellinger, S.L., McNeil, W.J., Unruh, T.C., McGregor, D.S., 2007. Angular Response of Perforated Silicon Diode High Efficiency Neutron Detectors. IEEE Nucl. Sci. Sym. Conf. Rec., 1904–1907.

Bellinger, S.L., McNeil, W.J., Unruh, T.C., McGregor, D.S., 2009c. Characteristics of 3D Micro-Structured Semiconductor High Efficiency Neutron Detectors. IEEE Trans. Nucl. Sci. 56, 742–746.

Dingley, J., Danon, Y., LiCausi, N., Lu, J.-Q., Bhat, I.B., 2010. Directional Response of Microstructure Solid State Thermal Neutron Detectors. In: Transactions of the American Nuclear Society and Embedded Topical Meeting Isotopes for Medicine and Industry 103, pp. 1190–1191.

Henderson, C.M., Jahan, Q.M., Dunn, W.L., Shultis, J.K., McGregor, D.S., 2010. Characterization of Prototype Perforated Semiconductor Neutron Detectors. Radiat Phys Chem, 144–150.

McGregor, D.S., Bellinger, S.L., Bruno, D., McNeil, W.J., Patterson, E., Rice, B.B., 2007. Perforated Semiconductor Neutron Detector Modules. In: Proceedings of the 32nd Annual GOMAC Technical Conference.

McGregor, D.S., Bellinger, S.L., McNeil, W.J., Unruh, T.C., 2008. Micro-Structured High-Efficiency Semiconductor Neutron Detectors. IEEE Nucl. Sci. Sym. Conf. Rec., 446–448.

McGregor, D.S., Hammig, M.D., Gersch, H.K., Yang, Y.-H., Klann, R.T., 2003. Design Considerations for Thin Film Coated Semiconductor Thermal Neutron Detectors. Part I: Basics Regarding Alpha Particle Emitting Neutron Reactive Films. Nucl. Instrum. Meth. A500, 272–308.

McGregor, D.S., Klann, R.T., 2003. Pocked Surface Neutron Detector. In: U.S.P.T.O. (Ed.), USA.

McGregor, D.S., Klann, R.T., 2007. High-Efficiency Neutron Detectors and Methods of Making the Same. In: U.S.P.T.O. (Ed.), USA.

McGregor, D.S., Klann, R.T., Gersch, H.K., Ariensanti, E., Sanders, J.D., VanDerElzen, B., 2002. New Surface Morphology for Low Stress Thin-Film-Coated Thermal-neutron Detectors. IEEE Trans. Nucl. Sci. 49, 1999–2004.

McGregor, D.S., McNeil, W.J., Bellinger, S.L., Unruh, T.C., Shultis, J.K., 2009. Microstructured Semiconductor Neutron Detectors. Nucl. Instrum. Meth. A608, 125–131.

McGregor, D.S., Shultis, J.K., 2011. Reporting Detection Efficiency for Semiconductor Neutron Detectors: A Need for a Standard. Nucl. Instrum. Meth. A632, 167–174.

McNeil, W.J., 2010. Perforated Diode Neutron Sensors. Kansas State University, Manhattan, KS.

McNeil, W.J., Bellinger, S.L., Unruh, T., Patterson, E., Egly, A., Bruno, D., Elazegui, M., Streit, A., McGregor, D.S., 2006. Perforated Diode Fabrication for Neutron Detection. IEEE Nucl. Sci. Sym. Conf. Rec., 3732–3735.

McNeil, W.J., Bellinger, S.L., Unruh, T.C., Henderson, C.M., Ugorowski, P.B., Dunn, W.L., Taylor, R.D., Blalock, B.J., Britton, C.L., McGregor, D.S., 2009a. 1024-Channel Solid State 1-D Pixel Array for Small Angle Neutron Scattering. In: Proceedings of the IEEE Nuclear Science Symposium Conference Record, Orlando, Florida, pp. 2008–2011.

McNeil, W.J., Bellinger, S.L., Unruh, T.C., Henderson, C.M., Ugorowski, P.B., Morris-Lee, B., Taylor, R.D., McGregor, D.S., 2009b. 1-D Array of Perforated Diode Neutron Detectors. Nucl. Instrum. Meth. A604, 127–129.

Nikolic, R.J., Conway, A.M., Radev, R., Shao, Q., Voss, L., Wang, T.F., Brewer, J.R., Cheung, C.L., Fabris, L., Britton, C.L., Ericson, M.N., 2010. Nine Element Si-based Pillar Structured Thermal Neutron Detector. Proc. SPIE—Int. Soc. Opt. Eng., 78050.

Nikolic, R.J., Conway, A.M., Reinhardt, C.E., Graff, R.T., Wang, T.F., Deo, N., Cheung, C.L., 2007. Fabrication of pillar-structured thermal neutron detectors. IEEE Nucl. Sci. Sym. Conf. Rec., 1577–1580.

Shultis, J.K., McGregor, D.S., 2004a. Efficiencies of Coated and Perforated Semiconductor Neutron Detectors. IEEE Nucl. Sci. Sym. Conf. Rec. 7, 4569–4574.

Shultis, J.K., McGregor, D.S., 2004b. Spectral Identification of Thin-Film-Coated and Solid-Form Semiconductor Neutron Detectors. Nucl. Instrum. Meth. A517, 180–188.

Shultis, J.K., McGregor, D.S., 2006. Efficiencies of Coated and Perforated Semiconductor Neutron Detectors. IEEE Trans. Nucl. Sci. 53, 1659–1665.

Shultis, J.K., McGregor, D.S., 2008. Designs for Micro-Structured Semiconductor Neutron Detectors. Proc. SPIE—Int. Soc. Opt. Eng., 707906–707915.

Shultis, J.K., McGregor, D.S., 2009. Design and Performance Considerations for Perforated Semiconductor Thermal-Neutron Detectors. Nucl. Instrum. Meth. A606, 608–636.

Solomon, C.J., 2007. Analysis and characterization of perforated neutron detectors. Manhattan, KS.

Solomon, C.J., Shultis, J.K., McGregor, D.S., 2010. Reduced Efficiency Variation in Perforated Neutron Detectors with Sinusoidal Trench Design. Nucl. Instrum. Meth. A618, 260–265.

Uher, J., Frojdh, C., Jakubek, J., Kenney, C., Kohout, Z., Linhart, V., Parker, S., Petersson, S., Pospisil, S., Thungstrom, G., 2007. Characterization of 3D Thermal Neutron Semiconductor Detectors. Nucl. Instrum. Meth. A576, 32–37.